

## Cooperativity of the $\beta$ -relaxations in aromatic polymers

Alejandro Sanz,<sup>1</sup> Aurora Nogales,<sup>1,\*</sup> Tiberio A. Ezquerra,<sup>1</sup> Nadia Lotti,<sup>2</sup> and Lara Finelli<sup>2</sup>

<sup>1</sup>*Instituto de Estructura de la Materia, C.S.I.C. Serrano 121, Madrid 28006, Spain*

<sup>2</sup>*Dipartimento di Chimica Applicata e Scienza dei Materiali, Università di Bologna, Via Risorgimento, 2, 40136 Bologna, Italy*

(Received 20 February 2004; published 10 August 2004)

The dielectric loss spectra of a series of copolyesters of poly(ethylene terephthalate) and poly(ethylene isophthalate) have been measured as a function of temperature in a broad frequency range ( $10^{-1}$ – $10^9$  Hz). By these measurements, the merging of the two relevant relaxations  $\alpha$  and  $\beta$  has been studied. The  $\beta$  processes exhibit a complex temperature dependence, showing a clear Arrhenius dependence at temperatures well below the glass transition temperature, a transition zone where the characteristic relaxation time of this process nearly does not change with temperature, and an Arrhenius behavior with a higher activation energy for temperatures above the glass transition. The analysis of these results indicates that the  $\beta$  relaxation in these systems presents typical characteristics of a genuine Johari-Goldstein process. This finding has been interpreted as due to the full monomer extension of the molecular motions involved in the  $\beta$  relaxation in agreement with recent proposals.

DOI: 10.1103/PhysRevE.70.021502

PACS number(s): 64.70.Pf, 77.22.Gm

### INTRODUCTION

Among the intriguing phenomena associated with the glass transition is the existence of an  $\alpha$  relaxation dominating the relaxation map of glass forming systems [1]. This process is manifested at temperatures above the glass transition temperature ( $T_g$ ), and it is associated with the cooperative reorientations and/or translations of the relaxing species. When the glass forming system is a polymer, the  $\alpha$  relaxation is attributed to cooperative segmental rearrangements in the main chain. However, in the relaxation map, there is also a weaker process that appears at higher frequencies and is usually denoted as  $\beta$  relaxation [1]. The  $\beta$  relaxation can be detected even below  $T_g$ . Traditionally, the  $\beta$  relaxation was assigned to local motions of only a part of the molecule and therefore it was considered to play no role on the  $\alpha$  process. However, the discovery by Johari and Goldstein of  $\beta$  relaxations in low-molecular-weight rigid molecules indicated that in some systems the  $\beta$  process involved the whole molecule. In these cases, the  $\beta$  relaxation is referred to as Johari-Goldstein (JG) relaxation [2]. According to Johari [3], structural nonuniformity within the glass leads to heterogeneity in mobility. The secondary process occurs in the regions where the mobility is higher. Recently, the relaxation time of the JG process has been found to be empirically related to the primitive relaxation time of the coupling model (CM), which is the precursor of the  $\alpha$  relaxation [4]. The CM provides a relation to estimate the characteristic relaxation time for the predicted primitive relaxation,

$$\tau_0 = (t_c)^n (\tau_\alpha)^{1-n}, \quad (1)$$

where  $\tau_\alpha$  in Eq. (1) is the characteristic relaxation time of the  $\alpha$  process,  $t_c$  is the crossover time from independent to cooperative relaxation and has been estimated to be  $2 \times 10^{-12}$  sec from neutron scattering experiments [5], and  $n$  is related to the exponent in the Kolraush function:

$$\phi(t) = \exp[-(t/\tau_\alpha)^{1-n}]. \quad (2)$$

If this primitive relaxation is responsible for the existence of the secondary process, it is expected that its characteristic time  $\tau_0$  is approximately the same as the characteristic time of the  $\beta$  relaxation,  $\tau_\beta$ . This approach has been shown to be valid for a great variety of low molecular glass forming [4,6] and polymer networks [7]. In polymer systems the  $\beta$  relaxation is independent of the  $\alpha$  process when it is due to localized motions of side chains and lateral pendant groups [6]. In these cases, the  $\beta$  relaxation bears no similarity with the concept of JG relaxation. However, it has been recently shown that for polymers without pendant groups or side chains, like, for example, 1,4-polybutadiene, or 1,4-polyisoprene, the  $\beta$  relaxation involves the whole monomeric repeat unit [8]. Therefore, even if the  $\beta$  relaxation may involve different intramolecular motions, when it affects essentially all atoms of the repeat unit, it can be envisioned as a JG process as shown by a recent report [6].

The improvement in resolution and the possibility of measuring in broader frequency ranges has provided the possibility of studying in more detail this weaker  $\beta$  relaxation. Based on previous molecular dynamics simulations [9], Boyd and Bravard [10] have proposed that the  $\beta$  relaxation in a paradigmatic aromatic polymer like poly(ethylene terephthalate) (PET), as studied by dielectric spectroscopy, is a complex process that can be deconvoluted into three different contributions, each of them associated with the motion of three different bonds involving essentially the whole monomeric unit. They remark that, in comparison with poly(ethylene 2,6-naphthalene dicarboxylate) (PEN) with identical chemical structure to that of PET with the exception of the phenyl group of PET being substituted in PEN by a naphthalene group, a particular component of the  $\beta$  process (the one appearing at lower frequencies) may have slight intrasegmental cooperative character.

With these ideas in mind, we have attempted to understand the connection between the  $\alpha$  and  $\beta$  relaxations and to probe the possible cooperative nature of the  $\beta$  relaxation. To achieve that, we have selected a series of random copolymers

\*Corresponding author.

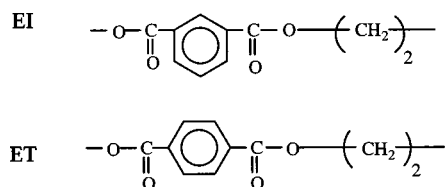


FIG. 1. Chemical structure of the monomers corresponding to the studied polymeric systems.

of PET and poly(ethylene isophthalate) (PEI). The chemical structure of the investigated samples is presented in Fig. 1. The ethylene isophthalate units provide the same ester groups to the macromolecular chains than the ones in the ethylene terephthalate units. However, due to its chemical nature and to the formation of copolymers, this family allows us to explore the coalescence between the  $\alpha$  and  $\beta$  processes at very high temperature, avoiding the crystallization of the systems. As a matter of fact, the rate of crystallization of both PET and PEI was found to be strongly depressed by copolymerization [11]. The interrelation between the secondary and the  $\alpha$  process in this series of copolymers has been studied in a broad-frequency-range dielectric spectroscopy, in order to shed some light on the role of the secondary process in glass forming polymers.

### EXPERIMENTAL PART

All the samples were synthesized according to the well-known two-stage polycondensation procedure. In order to obtain the two homopolymers and the copolymer family with different relative composition, several amounts of dimethyl terephthalate, dimethyl isophthalate, and ethylene glycol were used employing  $\text{Ti}(\text{O}i\text{Bu})_4$  as a catalyst [11]. The obtained copolymers are statistical, and in all cases the weight average molecular weight is around  $M_w = 50.000$  g/mol. The molar composition and the chain structure of the samples were determined by means of  $^1\text{H-NMR}$  spectroscopy [11]. The nomenclature used in this work to identify samples with different content of ethylene terephthalate units is presented in Table I. After vacuum drying at 363 K for 24 h, the powders originated from the synthesis were melt pressed at 560 K for 2 min and subsequently quenched to room temperature using water refrigerated metal blocks. In that way polymer films of about  $250 \mu\text{m}$  were obtained.

TABLE I. Nomenclature used in the present work, molar fraction of ET units,  $T_g$  of the samples as measured by DSC, and  $T_0$  and  $D$  obtained from the fittings of  $F_{\text{max}}^\alpha$  to Eq. (5).

Sample name	Molar fraction		$T_g$ (K)	$T_0$ (K)	D
	ET units				
ET100 (PET)	1.0		350	308	4.7
ET80	0.8		345	293	5.8
ET60	0.6		343	283	6.7
ET40	0.4		339	274	7.5
ET20	0.2		337	270	7.9
ET00 (PEI)	0.0		335	264	8.5

Films for dielectric spectroscopy were provided with circular gold electrodes (2 cm diameter for the low-frequency-range experiments and 0.5 cm diameter for the high-frequency range) by sputtering the metal onto both free surfaces. In some particular cases, (low ET content) Kapton spacers  $120 \mu\text{m}$  thick were used to avoid the two electrodes to collapse at high temperatures. DSC experiments were carried out using a Perkin-Elmer DSC4 instrument provided with an ethanol cooling bath. The temperature was calibrated by using indium. The samples were encapsulated in aluminum pans, and the typical sample weights used in these experiments were about 6 mg. The heating rate employed was 10 K/min. Dielectric loss measurements  $\epsilon'' = \text{Im}(\epsilon^*)$ , where  $\epsilon^*$  is the complex dielectric permittivity, were performed over a broad frequency window  $10^{-1} < F$  (Hz)  $< 10^9$  in a temperature range of  $123 < T$  (K)  $< 473$ . To cover the above frequency range, two different experiment setups were used. From  $10^{-1}$  to  $10^6$  Hz a Novocontrol system integrating an ALPHA dielectric interface was employed. In the range  $10^6$ – $10^9$  Hz, dielectric measurements were obtained by means of an HP 4291 coaxial line reflectometer. In this case, the dielectric loss was calculated by measuring the reflection coefficient at a particular reference plane [1,12]. These two instruments are integrated in a Novocontrol broadband dielectric spectrometer. The temperature in this spectrometer is controlled by a nitrogen jet (QUATRO from Novocontrol) with a temperature error, during every single sweep in frequency, of 0.1 K.

### RESULTS

Figure 2 shows, as an example, for four selected samples, the corresponding  $\epsilon''$  values as a function of frequency for temperatures at  $T > T_g$ . In the dielectric loss spectra of all the studied samples it is possible to distinguish two relaxation processes in different temperature regions. At low frequencies, a prominent maximum, assigned to the  $\alpha$  relaxation is observed together with a faster  $\beta$  process located at higher frequencies. For the temperatures near  $T_g$  the  $\alpha$  process appears well separated from the  $\beta$  one. However, as temperature increases, both relaxations exhibit very different dynamic-temperature dependence, and hence there is a progressive merging. At high enough temperatures, only a single  $\epsilon''$  maximum is observed in those samples in which crystallization is prevented (ET  $< 0.8$ ).

The relaxation curves as a function of frequency were analyzed according to the Havriliak-Negami (HN) formalism. In this case, the main features appearing in a typical dielectric loss ( $\epsilon''$ ) frequency scan can be phenomenologically described as the superposition of two HN processes and a conductivity term as follows:

$$\epsilon'' = \left( \frac{\sigma}{\epsilon_0 \omega} \right)^s + \text{Im} \left( \sum_{k=\beta, \alpha} \frac{\Delta \epsilon_k}{[1 + (i\omega \tau_{\text{HN } k})^{b_k}]^{c_k}} \right), \quad (3)$$

where  $\sigma$  is the direct current electrical conductivity,  $\epsilon_0$  is the vacuum permittivity, the coefficient  $0 < s < 1$  depends on the conduction mechanism [1,13],  $\omega$  is the angular frequency ( $\omega = 2\pi F$ ),  $\Delta \epsilon$  is the dielectric strength of the relaxation,  $\tau_{\text{HN}}$

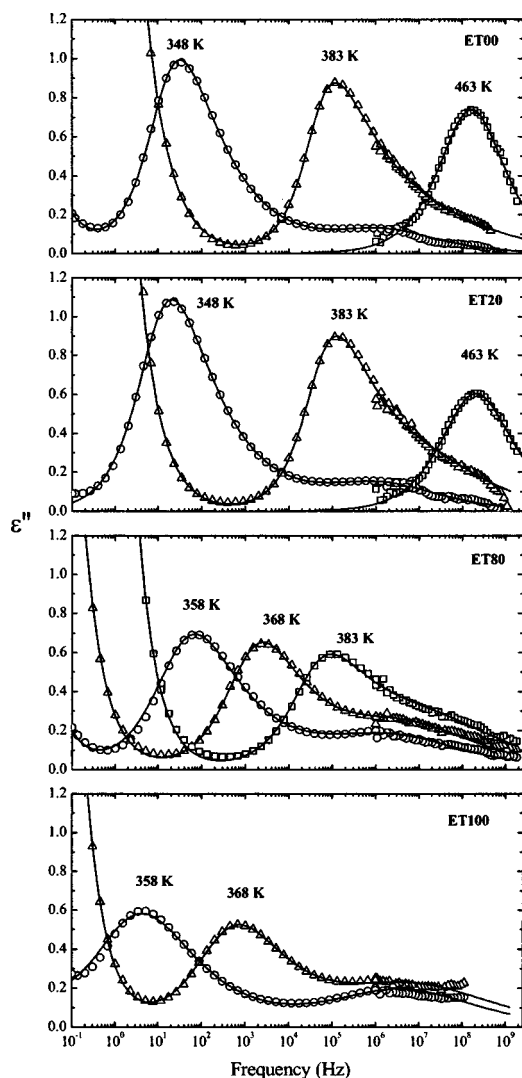


FIG. 2. Dielectric loss relaxation spectra as a function of frequency for selected temperatures, as indicated by the labels, presented for four samples [ET00(PEI), ET20, ET80, and ET100 (PET)]. The two main relaxation processes  $\alpha$  and  $\beta$  are observed. Solid lines represent best fits according to Eq. (3).

is the most probable value of the relaxation time distribution function, and  $b$  and  $c$  are shape parameters related to the symmetric and asymmetric broadening, respectively [1,14]. The central relaxation time  $\tau$  has been calculated as being

$$\tau = \frac{1}{2\pi F_{\max}} = \tau_{\text{HN}} \left[ \sin \frac{b\pi}{2+2c} \right]^{-1/b} \left[ \sin \frac{bc\pi}{2+2c} \right]^{1/b}, \quad (4)$$

where  $F_{\max}$  is the frequency of maximum loss. This sort of addition method has been successfully applied for describing experiment data on the merging of the  $\beta$  and  $\alpha$  relaxations [15–17].

Figure 3 shows as an example the separation procedure of the mentioned contributions to  $\epsilon''$  for the case of the ET80 sample measured at  $T=363$  K. The solid line represents the best fit obtained by a Gauss-Newton fitting procedure [18]. Dotted lines represent the isolated conductivity term and the

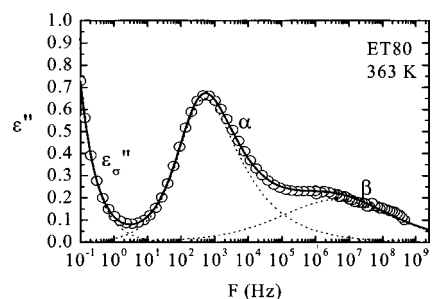


FIG. 3. Dielectric loss values for ET80 sample at  $T=363$  K. The solid line corresponds to the best fitting from Eq. (3). Dotted lines show the separated contribution of the conductivity term ( $\epsilon''_{\text{cond}}$ ) and the  $\beta$  and  $\alpha$  relaxation, respectively.

separated  $\beta$  and  $\alpha$  processes. At high temperature, the  $\beta$  relaxation maximum is located near the edge of the frequency window.

The variation of the obtained HN parameters as a function of temperature is presented in Fig. 4. As a general trend, in the whole copolymer series, the HN parameters for the  $\alpha$  and  $\beta$  contributions present a similar evolution with temperature.

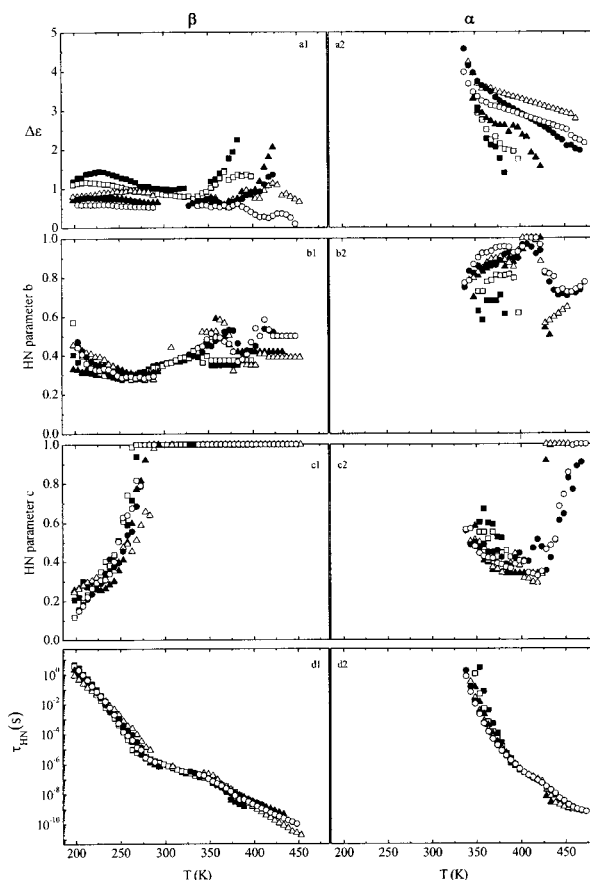


FIG. 4. Havriliak-Negami parameters obtained for the whole copolymer series corresponding to the  $\beta$  (left panels) and  $\alpha$  (right panels) relaxations: dielectric strength  $\Delta\epsilon$  ( $a_1$  and  $a_2$ ), symmetric broadening parameter  $b$  ( $b_1$  and  $b_2$ ), asymmetric broadening  $c$  ( $c_1$  and  $c_2$ ), and central relaxation time  $\tau_{\text{HN}}$  ( $d_1$  and  $d_2$ ). Different symbols corresponds to different ET comonomer concentration. (■) ET100 (PET), (□) ET80, (▲) ET60, (△) ET40, (●) ET20, and (○) ET00 (PEI).

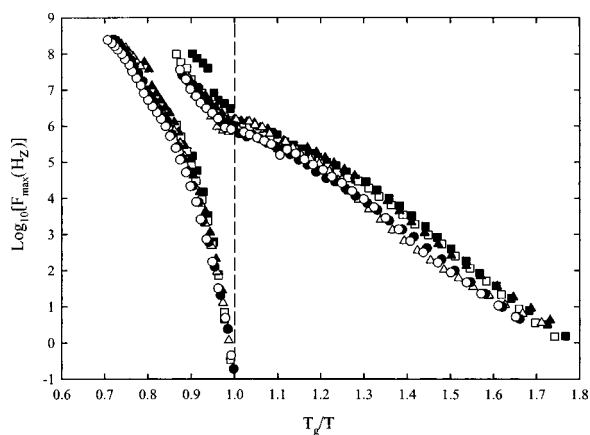


FIG. 5. Evolution of the frequency of maximum loss of the  $\alpha$  and  $\beta$  relaxations as a function of the reciprocal temperature, normalized by the calorimetric glass transition of each sample ( $T_g/T$ ). Same symbols as in Fig. 4.

The strength of the  $\beta$  relaxation ( $\Delta\varepsilon_\beta$ ) remains nearly constant for all the samples for temperatures below their calorimetric  $T_g$  and increases at higher temperatures. At even higher temperatures, PEI and the samples with low ET content show a further tendency of  $\Delta\varepsilon_\beta$  to decrease. The shape of the  $\beta$  relaxation changes with temperature. The symmetric broadening parameter  $b_\beta$  in the temperature measured range takes a value around 0.4. However, the asymmetric broadening  $c_\beta$  starts from very low values ( $\sim 0.2$ ) at low temperatures, indicating that in this range the  $\beta$  relaxation is asymmetric, and gradually increases with temperature up to the

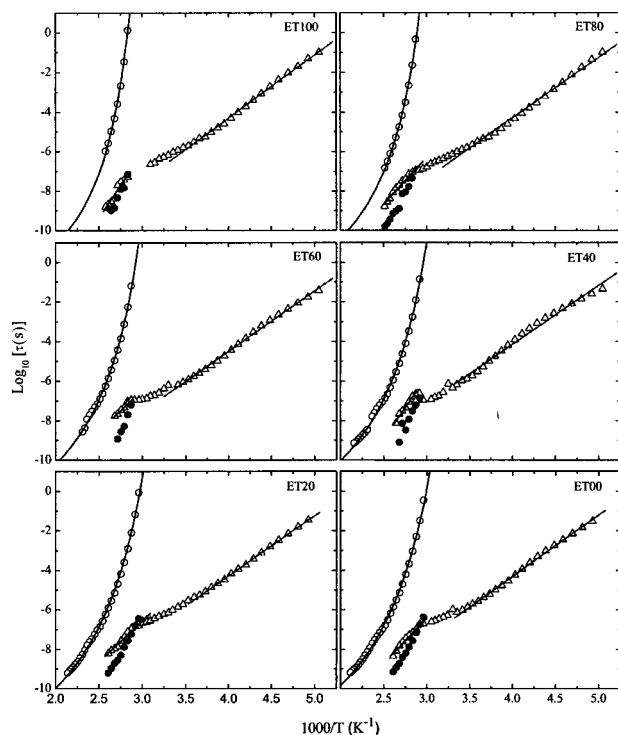


FIG. 6. Dependence of the central relaxation times of the  $\alpha$  [ $\tau_\alpha$  (O)] and  $\beta$  [ $\tau_\beta$  ( $\Delta$ )] processes for all the samples. Also, calculated primitive relaxation time  $\tau_0$  ( $\bullet$ ) obtained according to Eq. (1).

maximum value ( $c_\beta=1$ ) and for temperatures above  $\sim 275$  K the  $\beta$  process becomes symmetric. The central relaxation time  $\tau_{HN,\beta}$  decreases with temperature. This tendency is also observed for  $\tau_{HN,\alpha}$ . As opposed to  $\Delta\varepsilon_\beta$ ,  $\Delta\varepsilon_\alpha$  decreases with temperature in the whole range.  $b_\alpha$  values are between 0.6 and 1 in all the samples, showing moderate dispersion in the measured temperature window. The  $\alpha$  relaxation becomes more symmetric at higher temperatures as indicated by the upwards trend in the  $c_\alpha$  parameter. Above  $T \approx 450$  K the  $\alpha$  and  $\beta$  relaxations merge and the experimental data can be described by a single relaxation process.

### Temperature revolution of the different relaxations

As mentioned above,  $\alpha$  and  $\beta$  relaxations exhibit very different frequency-temperature behavior. In Fig. 5 the frequency of maximum loss ( $F_{\max}$ ) of each relaxation has been presented as a function of the reciprocal temperature in an Arrhenius-like representation. For the sake of clarity the reciprocal temperature has been normalized, for each sample, to its calorimetric glass transition. As can be observed, at low temperatures, the dependence of the  $F_{\max}^\beta$  with the reciprocal temperature tends to be linear, which corresponds to a typical Arrhenius behavior with an activation energy of  $59 \pm 1$  kJ/mol. This behavior is indicated in Fig. 6 by the solid straight line. However, at temperatures below, but very close to, the  $T_g$  of each sample,  $F_{\max}^\beta$  exhibits a nearly independent temperature behavior and in the range  $T > T_g$  a second Arrhenius-like dependence is observed, with a higher activation energy than the one at low temperatures. The  $F_{\max}^\alpha$  shows a homogeneous temperature evolution that in the Arrhenius representation exhibits some curvature which can be described with the Vogel-Fulcher-Tamman equation

$$F_{\max} = F_0 e^{-\frac{DT_0}{T-T_0}}, \quad (5)$$

where  $F_0$  is the preexponential factor,  $D$  is a parameter related to the fragility parameter [19], and  $T_0$  is the Vogel temperature. The curved solid lines in Fig. 6 represent the best fit according to Eq. (5) and the obtained parameters are presented in Table I. It is noteworthy that the fits have been performed considering  $F_0$  as  $1/(2\pi\tau_{\text{ANGELL}})$  where  $\tau_{\text{ANGELL}}$  is equal to  $10^{-14}$  s [19]. As can be observed from the parameters in Table I,  $T_0$  follows a similar trend to the one of  $T_g$ , being in all cases approximately 50 K lower. The  $D$  parameter slightly decreases as the ET content increases, indicating a subtly more fragile behavior in the case of PET than in the case of PEI.

### DISCUSSION

As mentioned in the Introduction, the center of interest of this work is to establish possible connections between the two main relaxation processes ( $\alpha$  and  $\beta$ ) appearing in aromatic polyesters and to find some cooperativity signature in the faster process ( $\beta$  one).

The more important facts with this respect found in the results of this work are the following. The temperature dependence of the  $\beta$  relaxation is more complex than the expected from a simple Arrhenius behavior. As observed from the relaxation map (Fig. 5),  $F_{\max}^\beta$  exhibits at least two

Arrhenius behaviors with very different slopes and a transition zone around  $T_g$  where  $F_{\max}^{\beta}$  remains nearly invariant to temperature. This invariability had been observed before for nonpolymeric glass formers [20], and it is a signature that  $\beta$  relaxation is strongly affected by the glass transition. This fact is also clearly observed in the dependence with temperature of the dielectric strength of the  $\beta$  process ( $\Delta\epsilon_{\beta}$ ) presented in Fig. 4(a) where a clear increase appears around at temperatures around the measured calorimetric  $T_g$ . These facts have important consequences in the interpretation of the  $\beta$  process. On the one hand, to assure that this sort of relaxations exhibits an Arrhenius-like behavior in the whole temperature range is incorrect or imprecise. Extrapolations of the Arrhenius tendency observed in the low-temperature range at temperatures above  $T_g$  may lead to inaccuracies when studying the merging of the  $\alpha$  and  $\beta$  processes as is clearly seen from our experimental results in broadband. Extrapolation of the linear behavior obtained in the Arrhenius plot at  $T < T_g$  would lead to a finite merging temperature ( $T_M > T_g$ ) where  $\tau_{\beta}$  becomes equal to  $\sigma_{\alpha}$ . According to some authors [21], this sort of behavior is one of the characteristic signatures of a  $\beta$  relaxation to be JG like. As mentioned in the previous section, at  $T > T_g$  the  $\beta$  relaxation exhibits a second Arrhenius dependence with a higher activation energy than the one at low temperatures. The new activation energies present some dispersion depending on the concentration of the studied copolyesters. This is due to the small number of points available for the fitting. However, in general, they are considerably higher than the one obtained at  $T < T_g$ , with an average value of 90 kJ/mol and a preexponential factor  $\tau_{\infty}$  around  $10^{-21}$  s. The fact that this extrapolation of  $\tau$  at very high temperatures provides a value faster than the phonon frequencies lacks of physical sense and as suggested by other authors provides an indication that the  $\beta$  process cannot continue to high temperatures ( $T \gg T_g$ ), but instead, it merges with the  $\alpha$  relaxation. This behavior is also typical of genuine JG relaxations and, in general, has been observed in low-molecular-weight glass forming liquids, by relaxation measurements under pressure. Here, due to the different behavior of the  $\alpha$  and  $\beta$  relaxations to this thermodynamic variable [21], both processes appear well separated. In our case, at ambient pressure, due to the broadband of the measuring technique and the use of copolyesters to avoid the crystallization of PET, this change in the slope of  $\tau_{\beta}$  above and below  $T_g$  is clearly observed. At this point we will focus on the possible cooperativity of the  $\beta$  relaxations. As mentioned before, recently Boyd and Bravard [10] by means of dielectric spectroscopy measurements have concluded that the nature of the  $\beta$  relaxation in PET at low temperatures ( $T < T_g$ ) is complex and can be described by three different contributions. Based both on experiments and on previous molecular dynamics simulations on the same system [9], they associate each of the three components of the  $\beta$  relaxation with each of the three conformationally flexible bonds present in the PET monomer—i.e., the bond between the aromatic ring carbon (CA) to the ester carbon (C) (CA-C bond), the one between the ester ether oxygen (O) to the aliphatic carbon bond (C) (C-O bond), and the one between the aliphatic carbon-carbon (C-C bond). Therefore, they attribute the origin of the  $\beta$  relaxation in PET to a pure in-

tramolecular one involving only the local motion of parts of the molecule. These three processes can only be well resolved at very low temperatures ( $T \ll T_g$ ). Our results at  $T < T_g$  are in agreement with this view, because of the strong asymmetric character of the  $\beta$  relaxation, which can be interpreted as due to a composite nature. The interpretation of an intramolecular origin of the  $\beta$  processes would seem, at a first glance, opposite to the definition of a pure JG  $\beta$  relaxation. However, Boyd and Bravard [10] also indicate in their work that, from the three different molecularly originated components of the  $\beta$  process, the slowest, one corresponding to the CA-C bond has the highest rotational barrier and that the mechanism to produce this component, which they referred to as  $\beta_3$ , involves some degree of intrasegmental cooperativity in groups of bonds rotations or conformational jumps. Upon approaching  $T_g$  ( $T < T_g$ ), the three components tend to merge into a single one [10] and it is not possible to resolve each of them. According to the coupling model [4], the independent or primitive relaxation is the precursor of the cooperative  $\alpha$  relaxation. This characteristic of the independent relaxation of the CM is shared with the JG relaxation. Therefore, if our  $\beta$  relaxation has some JG character, the independent relaxation time  $\tau_0$ , defined in Eq. (1), should be located near  $\tau_{\beta}$ . Values of the KWW exponent were calculated after inverse Laplace transformation of the HN functions describing the  $\alpha$  relaxation and subsequent fitting to the KWW curve of the time-domain data [18]. We have calculated  $\tau_0$  for all the series of copolyesters measured and the results are presented in Fig. 6. As can be observed in these figures, the agreement between  $\tau_{\beta}$  and  $\tau_0$  at  $T > T_g$  is very good in the whole range and allows us to propose that, in PET and their analog isomers, the  $\beta$  relaxation possesses typical features of a pure JG relaxation at  $T > T_g$ . This can be understood as due to the intrasegmental cooperativity of the  $\beta$  relaxation derived from the full monomeric extension of the molecular components involved in it.

## CONCLUSIONS

In this work the complex temperature behavior of the  $\beta$  relaxation in aromatic copolyesters is reported. The more relevant and significant results are summarized in the following.

- (i) The onset of the glass transition affects markedly to the  $\beta$  relaxation.
- (ii) The shape of both processes is almost unaffected by the presence of structural isomers, being in all cases very similar to those of PET.
- (iii) At  $T > T_g$  the  $\beta$  relaxation in these systems exhibits specific features, which according to the coupling model, are characteristic of the primitive relaxation leading to the  $\alpha$  relaxation.

## ACKNOWLEDGMENTS

The authors thank the MCYT (Grant No. FPA2001-2139), Spain for generous financial support of this investigation. A. N. thanks the Ramon y Cajal program of the Spanish MCYT.

- [1] A. Schönhalz and F. Kremer, *Broad Band Dielectric Spectroscopy* (Springer-Verlag, Berlin, 2002).
- [2] G. P. Johari and M. Golstein, *J. Chem. Phys.* **53**, 2372 (1970).
- [3] G. P. Johari, *J. Chem. Phys.* **58**, 1766 (1973).
- [4] K. L. Ngai and K. Y. Tsang, *Phys. Rev. E* **54**, R3067 (1996).
- [5] J. Colmenero, A. Arbe, and A. Alegría, *Phys. Rev. Lett.* **71**, 2603 (1993).
- [6] K. L. Ngai and M. Paluch, *J. Chem. Phys.* **120**, 857 (2004).
- [7] V. Y. Kramarenko, T. A. Ezquerra, and V. P. Privalko, *Phys. Rev. E* **64**, 051802 (2001).
- [8] C. M. Roland, M. J. Schroeder, J. J. Fontanella, and K. L. Ngai, *Macromolecules* **37**, 2630 (2004).
- [9] R. H. Boyd and S. U. Boyd, *Macromolecules* **34**, 7219 (2001).
- [10] R. H. Boyd and S. P. Bravard, *Macromolecules* **36**, 741 (2003).
- [11] L. Finelli, M. Fiorini, V. Siracusa, N. Lotti, and A. Munari, *J. Appl. Polym. Sci.* (to be published).
- [12] T. A. Ezquerra, F. Kremer, and G. Wegner, in *Dielectric Properties of Heterogeneous Materials*, edited by A. Priou (Elsevier, Amsterdam, 1992), Vol. 6.
- [13] K. U. Kirst, F. Kremer, and V. M. Litinov, *Macromolecules* **26**, 975 (1993).
- [14] S. Havriliak and S. Negami, *Polymer* **8**, 161 (1967).
- [15] D. Gomez, A. Alegria, A. Arbe, and J. Colmenero, *Macromolecules* **34**, 503 (2001).
- [16] S. Kahle, J. Korus, E. Hempel, R. Unger, S. Höring, K. Schröter, and E. Donth, *Macromolecules* **30**, 7214 (1997).
- [17] R. Casalini and C. M. Roland, *Phys. Rev. Lett.* **91**, 15 702 (2003).
- [18] WinFit, Novocontrol GmbH (1996).
- [19] C. A. Angell, *Polymer* **38**, 6261 (1997).
- [20] N. B. Olsen, T. Christensen, and J. C. Dyre, *Phys. Rev. E* **62**, 4435 (2000).
- [21] M. Paluch, C. M. Roland S. Pawlus, J. Ziolo, and K. L. Ngai, *Phys. Rev. Lett.* **91**, 115701 (2003).